

Image Segmentation by Image Foresting Transform with Geodesic Band Constraints

Caio de Moraes Braz

Department of Computer Science
University of São Paulo (USP)
05508-090 - São Paulo - SP - Brazil
e-mail: caio**braz**@vision.ime.usp.br

Paulo André Vechiatto de Miranda

Department of Computer Science
University of São Paulo (USP)
05508-090 - São Paulo - SP - Brazil
e-mail: pmiranda@vision.ime.usp.br

Abstract—The Image Foresting Transform framework (IFT) was successfully used to implement several segmentation methods, including watersheds and fuzzy connectedness, however the lack of regularization terms in its formulation leads to a potential irregular (jagged) segmentation. An attempt to avoid this issue is to employ shape constraints that favor more regular shapes. We present a novel shape constraint, called the Geodesic Band Constraint (GBC) and show how it can be efficiently incorporated in the Image Foresting Transform framework, with its proof of optimality in terms of an energy function, subject to the new constraint. This constraint helps us to improve the segmentation of regular objects. The GBC can be also used with a prior shape template in order to drive the segmentation towards a specific shape with a single parameter that controls the degrees of freedom of the allowed deformations subject to the model.¹

I. INTRODUCTION

Image Segmentation consists of a partitioning of an image in multiple regions, such as to extract objects from a background, being useful in many domains such as medical and biological image analysis, edition and composition of natural images, optical character recognition, among others [1]. It is one of the core and most challenging problems in image processing and computer vision.

Given the discrete nature of digital images, the graph theory came as an appropriate tool to represent, compute and analyze images [2]. As a consequence, this area has attracted a lot of interest lately, as we can see from the rising quantity of papers published in the area [3], the congresses entirely dedicated on this subject and books exclusively dedicated to the topic [2].

Image segmentation can be formulated in graphs as an optimization problem of a graph-cut measure, such as the ε_∞ -minimization [4], [5]. Apart from the achieved success in many applications and the popularity of related approaches to the problem of the ε_∞ -minimization, such as watershed from markers [6]–[8], iterative relative fuzzy connectedness [9] and the Image Foresting Transform [7], the lack of regularization constraints make these methods not appropriate, for some applications domains. For example, when the expected shape of the object is simple or regular, the presence of defective segments on its border could generate issues in the form

of false positives or negatives, resulting not only in wrong segmentations but also with jagged borders (Figure 1a).

This work lies inside the problem of the ε_∞ -minimization of the Generalized Graph Cuts (GGC) [4], [5] and it is motivated by some recent breakthroughs such as the introduction of the Geodesic Star Constraint (GSC) in [10] on the Image Foresting Transform, resulting in the GSC-IFT [11]. In the context of the ε_∞ -minimization, this constraint removes undesired irregular shapes, improving the segmentation of more regular objects (Figure 1b), while keeping the low computational cost of the IFT. Based on this idea, we present a novel shape constraint, called Geodesic Band Constraint (GBC) and devise a new algorithm that efficiently implements the IFT subject to this constraint, called GBC-IFT.

The new algorithm computes a global optimal solution for the ε_∞ -minimization problem subject to the new constraint (Figure 1d). This constraint can be combined with GSC and border polarity constraints [12], [13], allowing a better management of the problem. The method can be also used with prior shape templates.

In Section II, we introduce some basic elements about digital images and the Image Foresting Transform, followed by our original contributions in Section III, where we introduce the Geodesic Band Constraint (GBC), in its absolute and relative variants. Finally, our conclusions are stated in Section IV.

II. BACKGROUND

A. Image Foresting Transform

In the IFT framework, an image can be seen as a directed graph $G = (\mathcal{I}, \mathcal{A})$ where the vertices are the image pixels in its domain $\mathcal{I} \subset \mathbb{Z}^n$ and the arcs are the ordered pairs of pixels $(s, t) \in \mathcal{A}$ defined by an adjacency relation \mathcal{A} . Each arc $(s, t) \in \mathcal{A}$ has a given weight $\omega(s, t) \geq 0$, that can be given by a measure of dissimilarity between pixels s and t , that usually depends on local features of image, such as color, gradient and vertex position.

A path $\pi_t = \langle t_1, t_2, \dots, t_n = t \rangle$ on this graph is a sequence of adjacent pixels ending at a pixel t . In this work, we consider only simple paths, that is, no vertex appears more than once. We use the notation $\pi_t = \langle t \rangle$ to indicate a single vertex path, namely the trivial path.

¹This work relates to a M.Sc. dissertation available at: <http://www.teses.usp.br/teses/disponiveis/45/45134/tde-01062016-104354/>

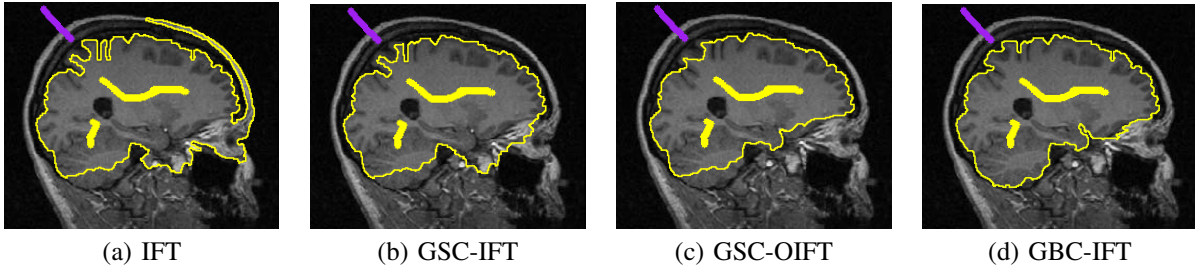


Fig. 1. Skull stripping examples, performed by different algorithms, for the same set of seeds.

In the IFT framework, we consider a predecessor map, a function P that associates to each node an adjacent one or a root marker. A spanning forest is cycle-free predecessor map P , that is, starting from any vertex and going back through the predecessors, we find a root marker in a finite number of iterations. A cost function f associates a cost value $f(\pi_t)$ to a path π_t on the graph. Usually this function is based on the arc weights along the path.

In the binary segmentation (two classes) via IFT with seed competition, we consider two sets of seeds, namely \mathcal{S}_o (object seeds) and \mathcal{S}_b (background seeds). Both sets compete trying to “conquer” further image pixels, so that this results in a partition of the image in two optimal-path forests, the former, rooted in object seeds, defining the object, and the latter rooted in background seeds, defining the background [7].

B. Geodesic Star Convexity

The importance of shape constraints in the IFT is due to the fact that resulting segmentations could be irregular. An avoidance measure to this issue is the employment of constraints to the object shape, such as the Geodesic Star Convexity (GSC), in order to filter undesired shapes. An object satisfies the GSC in relation to a center point c if for every object point p , every point in the line segment linking c to p also belongs to the object.

We consider the star centers as the object seeds chosen by the user and the line segments as paths leading each object point to its nearest star center, thus forming an IFT minimal geodesic path forest.

Note that any convex shape is also a star-convex shape, however not every star-convex shape is a convex one, thus making the GSC more versatile as shown in Figure 2.

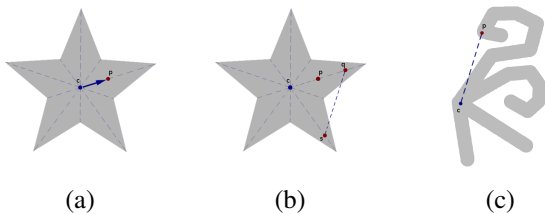


Fig. 2. Examples where we check the convexity constraint. Note that in (a) and (b) we show a shape that is star-convex but not convex.

C. Oriented Image Foresting Transform

The IFT can be also used when we model the image as a directed graph, where $\omega(s, t) \neq \omega(t, s)$, resulting in a method in which is possible to segment images favoring borders that have darker-to-brighter transitions or vice-versa.

In this situation is important to note that each segmentation defines two distinct graph cuts, one of them formed by arcs from background-to-foreground pixels and other from foreground-to-background pixels, namely inner cut (C_i) and outer cut (C_o), respectively.

As a consequence, two distinct energies arise, E_i and E_o , linked to C_i and C_o respectively, thus providing different resulting segmentations when optimized:

$$C_i(L) = \{(s, t) \in \mathcal{A} \mid L(s) = 0, L(t) = 1\} \quad (1)$$

$$C_o(L) = \{(s, t) \in \mathcal{A} \mid L(s) = 1, L(t) = 0\} \quad (2)$$

$$E_i(L) = \max_{(s, t) \in C_i(L)} \bar{\omega}(s, t) \quad (3)$$

$$E_o(L) = \max_{(s, t) \in C_o(L)} \bar{\omega}(s, t) \quad (4)$$

We can define specific cost functions in IFT, in order to obtain segmentations that minimize such energies and consequently favor transitions in the desired directions (brighter-to-darker or darker-to-brighter), as shown in Figure 3.

III. CONTRIBUTIONS

A. Geodesic Band Constraint

In this section we present our novel shape constraint, named Geodesic Band Constraint. The main idea consists in assigning a maximum limit (band width) for the variation of the geodesic cost between the points in the object border in order to avoid irregularities in the final delineation. We control the band width by means of a fixed parameter Δ , therefore it is possible to adjust the constraint.

Let \mathcal{O} be the set of object pixels and $\mathcal{B}(\mathcal{O})$ the set of pixels in its border, we then have:

Definition: Geodesic Band Constraint - GBC
An object \mathcal{O} satisfies the Geodesic Band Constraint with size Δ if $\forall t \in \mathcal{O}$ we have $C(t) \leq \min_{s \in \mathcal{B}(\mathcal{O})} C(s) + \Delta$.

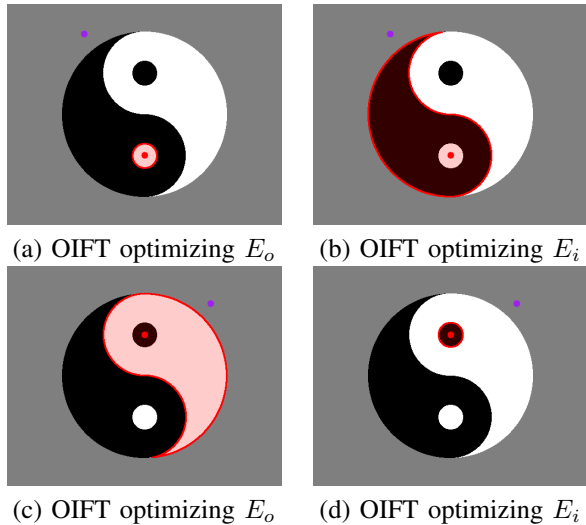


Fig. 3. OIFT example where we can see the differences when we choose our desired transition to favor. Note that we can change drastically the final result choosing a different energy function to optimize while keeping the same seed sets.

Our new method, that employs this shape constraint is called Geodesic Band Constraint IFT (GBC-IFT), and in summary, works as follows:

- 1) Generation of a Geodesic cost map C .
This first part consists in computing a optimal-path forest such that its roots are the initially defined object seeds. This is done by means of a IFT with an additive (geodesic) cost function. This forest is stored in a predecessor map P and the path values stored in a cost map C .
- 2) Segmentations with the Geodesic Band Constraint.
In this part, the segmentation itself occurs. It is made by a seed competition which checks if the GBC is being violated and fixes the border if such a violation occurs.

The GBC restricts the object border pixels in order to make sure that they are inside a fixed Δ sized band, preventing variations greater than this value thereby regularizing its shape. During the process, the band changes its position, allowing an adaptation to the image features (Figure 4). Note that only its position changes while its width is kept fixed.

A natural question that arises is how to estimate the adequate Δ for a given image. If it is too small, we risk to restrict the border too much, thus making the resulting segmentation not representative to the image contents; on the other hand a too large value will be innocuous since it will make the restriction so small that the method will degenerate in a simple IFT with no restriction whatsoever.

This choice problem can be tackled generating energy curves of the mean and maximum ε_∞ resulted from several values of Δ . With these values we can analyze for each image if there are segmentations that are robust to changes of Δ , detected by simultaneous flat lines on the mean and maximum energy curves. We name those the *stable segmentations*, and

a possible choice of Δ for them would be the one that yields more robustness to parameter changes.

We can also combine the GBC with other constraints, including the ones presented in Section II, in a similar way as done [13]. Joining the GBC with the GSC and border polarity, yielded a new method, called GBC-GSC-OIFT, that gave us more power to control some segmentation features, as shown in Figure 5.

B. Relative Geodesic Band Constraint

An evolution of the GBC consists in using a relative parameter p instead of the fixed parameter Δ to control the segmentation. In some cases, the fixed parameter Δ of the GBC-IFT prevents us from detecting variations that are relatively small but are big in absolute numbers. These features can help us to regularize some shapes, however can also prevent us from finding others, as we can see in Figure 6.

The fact that Δ is an absolute value, makes objects with different scales be compared by the same metric, potentially resulting in distinct segmentations, even from similar shapes contained in the same image, making the constraint not robust to the scale.

A way we found to prevent this issue is to specify a parameter p instead of Δ , making it relative to the minimum value found so far in the object border. This makes the band width proportional to the scale found in the process at each instant. With that, we can define the new constraint as:

Definition: Relative Geodesic Band Constraint - RGBC
An object \mathcal{O} satisfies the Relative Geodesic Band Constraint of proportion p if $\forall t \in \mathcal{O}$ we have $C(t) \leq \min_{s \in \mathcal{B}(\mathcal{O})} C(s) \cdot (1+p)$.

RGBC leads to an analog method of the GBC-IFT, called RGBC-IFT, presented in Figure 7.

C. Relative Geodesic Band Constraint with Shape Templates

We can also utilize predefined cost maps, obtained externally. In this case, the idea is to use some cost map C in the place of the one created by the method.

Once these cost maps are obtained, they are centralized on the “mass center” of the object seed set and then we execute the method normally after that. This drives our segmentation to the shape presented on the given cost map template (Figure 8), as exemplified in Figures 9 and 10.

IV. CONCLUSION

The geodesic band constraint was successfully incorporated on the ε_∞ -minimization framework by means of the development of a novel algorithm with its proof of correctness. In this algorithm we have a single parameter to control the constraint that can be defined as absolute (Δ) or relative (p).

As contributions then, we have the development and deployment of two novel methods (GBC-IFT and RGBC-IFT) and a paper published on the *2014 IEEE International Conference on Image Processing* [14].

A possible unfolding of this work consists in the study of a sense of locality on the proposed constraints. Currently, when

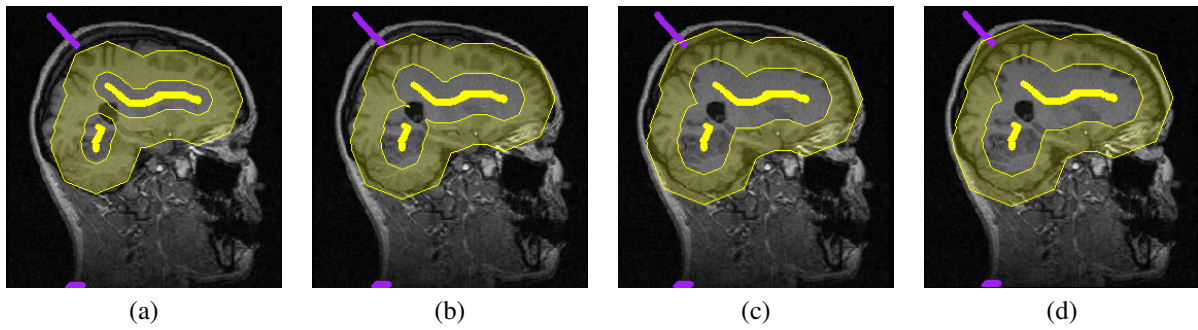


Fig. 4. (a-d) The fixed size band evolves starting from the seeds, adapting to the image contents. The delineated border (Figure 1d) is contained inside the band, helping us to avoid false segmentations.

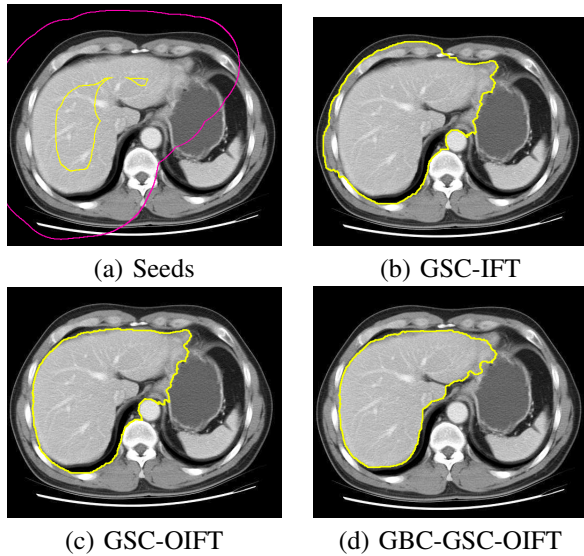
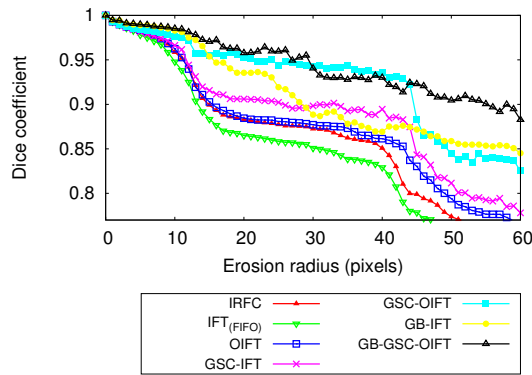


Fig. 5. Accuracy comparison between several segmentation methods for a CT image from a human liver, using the same set of seeds.

the constraint is violated, its correction is made globally in all the extension of the border, however, we try to limit these changes to a region closer to a given point of violation.

The proposed methods are extensible to 3D images and can be included in a automatic segmentation framework, in the cases where the seeds are available from an external source or when it is possible to generate them automatically.

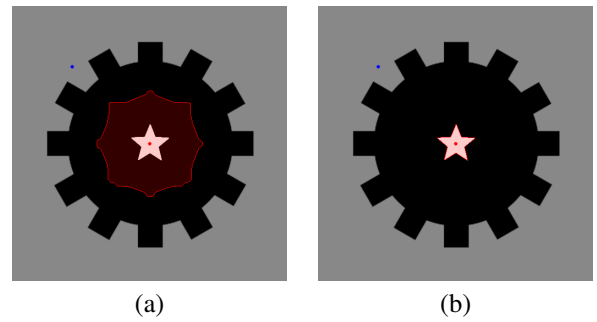


Fig. 6. Example showing how, for every Δ value, the GBC-IFT failed to segment the black gear.

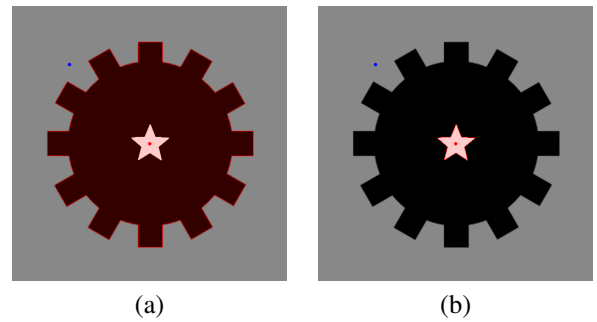


Fig. 7. Example showing how the RGBC-IFT was able to segment the black gear.

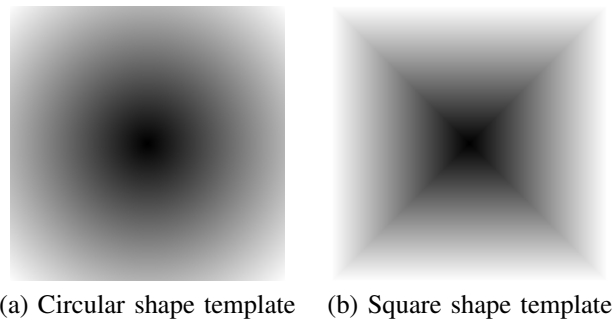
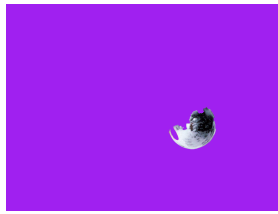


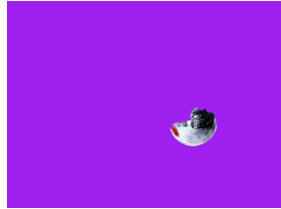
Fig. 8. Example of predefined shape templates that can be used as cost maps.



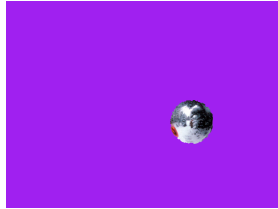
Seed markers in the image



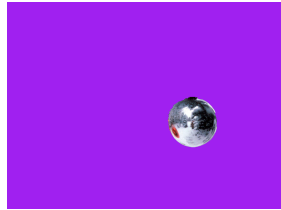
IFT



GSC-IFT



RGBC-IFT ($p = 0.05$)



RGBC-IFT ($p = 0.10$)



RGBC-IFT ($p = 0.20$)

Fig. 9. Segmentation example using the prior circle template.



Seed markers in the image



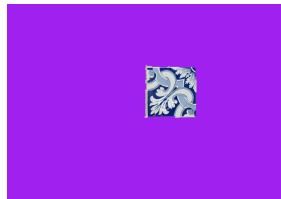
IFT



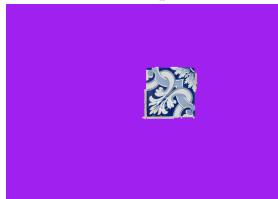
GSC-IFT



RGBC-IFT ($p = 0.05$)



RGBC-IFT ($p = 0.10$)



RGBC-IFT ($p = 0.20$)

Fig. 10. Segmentation example using the prior square template.

With our predefined shape templates, it is possible to analyze more complex shapes. We can also compare this technique with others that propose similar ideas with shape prior constraints [15] e [16]. In [15], for example, it uses a Gaussian Pyramid for the scale treatment while our method covers the scale automatically with the cost map with no additional computational cost, but we are yet to compare the accuracy of those methods for a given application.

ACKNOWLEDGMENTS

The authors thanks FAPESP grant # 2011/50761-2, CNPq, CAPES, NAP eScience - PRP - USP for financial support.

REFERENCES

- [1] R. Gonzalez and R. Woods, *Digital Image Processing*. Reading, MA, USA: Addison-Wesley, 1992.
- [2] O. Lézoray and L. Grady, *Image Processing and Analysis with Graphs: Theory and Practice*. California, USA: CRC Press, 2012.
- [3] K. S. Camilus and V. K. Govindan, "A review on graph based segmentation," *Intl. Journal of Image, Graphics and Signal Processing*, vol. 4, no. 5, pp. 1–13, 2012.
- [4] C. Couprie, L. Grady, L. Najman, and H. Talbot, "Power watersheds: A unifying graph-based optimization framework," *Trans. on Pattern Anal. and Machine Intelligence*, vol. 99, 2010.
- [5] K. Ciesielski, J. Udupa, A. Falcão, and P. Miranda, "A unifying graph-cut image segmentation framework: algorithms it encompasses and equivalences among them," in *Proc. of SPIE on Medical Imaging: Image Processing*, vol. 8314, 2012.
- [6] J. Cousty, G. Bertrand, L. Najman, and M. Couprie, "Watershed cuts: Thinnings, shortest path forests, and topological watersheds," *Trans. on Pattern Analysis and Machine Intelligence*, vol. 32, pp. 925–939, 2010.
- [7] P. Miranda and A. Falcão, "Links between image segmentation based on optimum-path forest and minimum cut in graph," *Journal of Mathematical Imaging and Vision*, vol. 35, no. 2, pp. 128–142, 2009.
- [8] R. Audigier and R. Lotufo, "Watershed by image foresting transform, tie-zone, and theoretical relationship with other watershed definitions," in *Proc. of the 8th Intl. Symposium on Mathematical Morphology and its Applications to Signal and Image Processing*, Oct 2007, pp. 277–288.
- [9] K. Ciesielski, J. Udupa, A. Falcão, and P. Miranda, "Fuzzy connectness image segmentation in graph cut formulation: A linear-time algorithm and a comparative analysis," *Journal of Mathematical Imaging and Vision*, 2012.
- [10] V. Gulshan, C. Rother, A. Criminisi, A. Blake, and A. Zisserman, "Geodesic star convexity for interactive image segmentation," in *Proc. of Computer Vision and Pattern Recognition*, 2010, pp. 3129–3136.
- [11] L. Mansilla, M. Jackowski, and P. Miranda, "Image foresting transform with geodesic star convexity for interactive image segmentation," in *Proceedings of the IEEE International Conference on Image Processing (ICIP)*, Set 2013, pp. 4054–4058.
- [12] P. Miranda and L. Mansilla, "Oriented image foresting transform segmentation by seed competition," *IEEE Transactions on Image Processing*, vol. 23, no. 1, pp. 389–398, 2014.
- [13] L. Mansilla and P. Miranda, "Image segmentation by oriented image foresting transform with geodesic star convexity," in *15th International Conference on Computer Analysis of Images and Patterns (CAIP)*, vol. 8047, 2013, pp. 572–579.
- [14] C. Braz and P. Miranda, "Image segmentation by image foresting transform with geodesic band constraints," in *Proceedings of the IEEE International Conference on Image Processing (ICIP)*, Oct 2014, pp. 4333–4337.
- [15] D. Freedman and T. Zhang, "Interactive graph cut based segmentation with shape priors," in *Computer Vision and Pattern Recognition, 2005. CVPR 2005. IEEE Computer Society Conference on*, vol. 1, June 2005, pp. 755–762 vol. 1.
- [16] N. Vu and B. Manjunath, "Shape prior segmentation of multiple objects with graph cuts," in *Computer Vision and Pattern Recognition, 2008. CVPR 2008. IEEE Conference on*, June 2008, pp. 1–8.